



Investigation of a Receiver-Tracked Parabolic Trough Concentrator

Ahlem HOUCINE, Taher MAATALLAH, Souheil EL ALIMI and Sassi BEN NASRALLAH
Laboratory studies of thermal and energy systems, Engineering Department, National Engineering School of
Monastir, Avenue Ibn Jazzar 5019 Monastir, Tunisia.

houcineahlem@yahoo.fr, maatallahtaher@yahoo.fr, souheil.elalimi@yahoo.fr, sassi.bennasrallah@enim.rnu.tn

ABSTRACT: The Parabolic Trough Concentrator is considered as the most mature and cost-effective power concentrated solar technologies. In fact, for several years, researchers are interested to investigate the PTC's efficiency taking account the shadow losses and its influences on the concentrated solar flux on the receiver area. In fact, the present study, basing on the RT 3D-4R technique, analyzes the shadow phenomena for different operational scenarios. Indeed, the hourly involved shadow phenomena are investigated for a blind PTC under the DNI of Monastir city, Tunisia. Moreover, the gain made by one-axis tracked PTC's system and receiver tracked one will be compared.

Keywords: RT 3D-4R method; shadow phenomena; one-axis tracked PTC system; receiver tracking system

1. Introduction

The stationary implementations, which kept the solar collector in a fixed position, have a compromised productivity, only, when the incident solar rays are in the reflector optimal angle [1]. Therefore, the performance of PTC can be improved and the collected amount of energy can be increasing by using solar tracking systems. The advantages of the tracking system is that very little collector adjustment is required during the day and the full aperture always faces the sun at noon time but the collector performance during the early and late hours of the day is greatly reduced due to large incidence angles [2]. Others advantages of using solar tracking system are mentioned by Gaafar et al. [3]. Many forms of tracking mechanisms, varying from complex to very simple, are presented in literature. They can be divided into two classes, namely electronic and mechanical systems [4-6]. In addition, as presented by Wang et al. [7], the PTC tracking system can be divided into two tracking techniques; single axis tracking and dual tracking systems. As the PTC reflective surface concentrated solar rays onto a receiver tube located along the trough single horizontal focal line, hence it is sufficient to track the sun along only one axis [8-10]. However, the dual axis tracker PTC system is usually used in locations where the sunlight is weaker than other parts of the world [11], even with the disadvantage of losing thermal energy and the not cost effective [12]. Another solar tracked system has been under study which is called the tracked receiver with a fixed reflector. This form of tracking consists to fix the reflector and only the receiver tube moves in order to track the reflected sun rays by the parabola surface.

In this paper, a developed ray tracing code called RT3D-4R is used to investigate the optical performance of a fixed PTC. In the first part, we are interesting to examine all the possible optical phenomena occurred by interactions between solar incident rays and both the reflector and receiver surfaces taking into account the shading effects. In the second part, we are investigating a novel (3D) model of tracking solar concentrator in which a cylindrical reflector in a place of parabolic trough one is considered and the focal length is not fixed but varies as function of the bilateral displacement of the centerline of the heat tube receiver. Indeed, we will compare the optical concentration characteristics of this new design with the one-axis PTC system.

2. Physical model

The PTC, as shown in Fig.1, is composed by a parabolic reflective surface and a coated absorber tube covered by glass. In this paper, the incident solar irradiation is considered as a ray package, defined by the optic

cone where $\sigma_{sun} = 32'$ [13]. Also, the solar-optical properties of the PTC system (ρ_s , τ_{eff} and α_{eff}) are assumed to be equal to the unit and independent of the temperature and the incidence angle.

2.1 Geometric parameters

Fig. 1 specifies the coordinate system used for describing the PTC solar system. As presented by Houcine et al. [14], the PTC geometric parameters used in this paper are illustrated in table 1

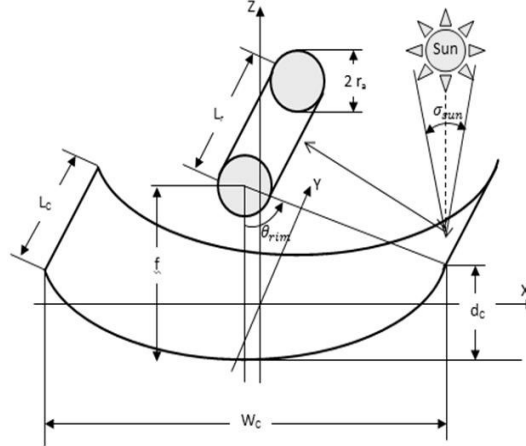


Figure 1: Schematic diagram of the PTC coordinate system, shown in 3D

Table 1: geometric parameters of PTC

	Parameter	value
Parabolic trough reflector	w_c	5 m
	l_c	7.8 m
	f	1.25 m
Receiver	r_a	0.035 m
	l_r	7.8 m

The equation of the parabola reflector is expressed as follows:

$$z = \frac{x^2}{4f} \quad (1)$$

The equation of the absorber tube is expressed as follows:

$$(x - x_{cr})^2 + (z - z_{cr})^2 = r_a^2 \quad (2)$$

2.2. Heat density

The heat receiver energy of each element surface from the collector can be calculated basing on the following expression

$$Q_s = \xi_s \cdot dS \cdot \vec{i} \cdot \vec{n} \quad (3)$$

Considering a four collector sampling points $M_c(i, j)$, $M_c(i+1, j)$, $M_c(i, j+1)$ and $M_c(i+1, j+1)$, the heat solar energy concentrated by an elementary sunspot on the reflector can be expressed as the following:

$$Q_s(i, j) = \xi_s \left[y_c(i, j+1) - y_c(i, j) \right] \left[x_c(i+1, j) - x_c(i, j) \right] \left[\frac{x_c(i+1, j) - x_c(i, j)}{4f} x_i - z_i \right] \quad (4)$$

The heat density on the surface of the receiver is $ds(i, j, \dot{i}_r, \dot{j}_r) = \frac{Q_s(i, j)}{ds_r(\dot{i}_r, \dot{j}_r)}$ in the light

spot surface and $ds(i, j, \dot{i}_r, \dot{j}_r) = 0$ elsewhere.

The total heat density of the receiver is:

$$D(\dot{i}_r, \dot{j}_r) = \sum_{\dot{i}_r, \dot{j}_r} ds(i, j, \dot{i}_r, \dot{j}_r) \quad (5)$$

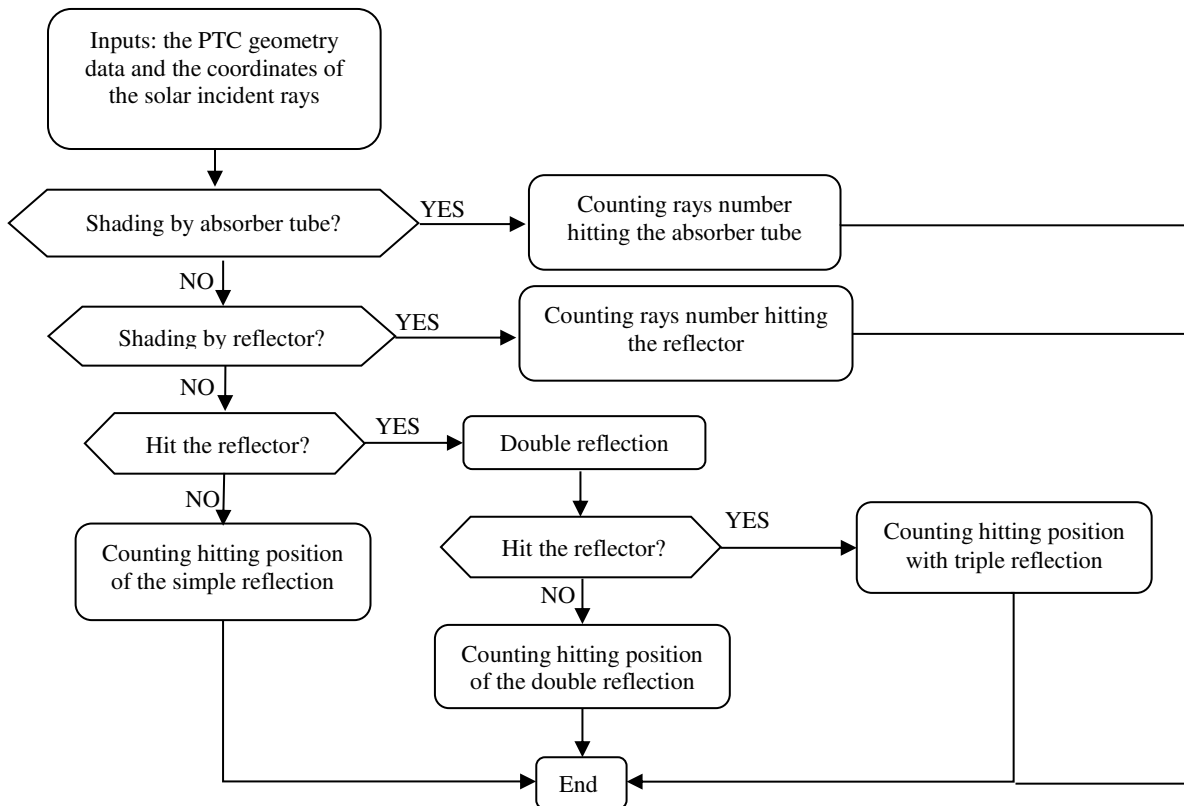
2.3. Simulation method

The proposed numerical method is inspired from the ray tracing techniques and it is called RT3D-4R. The method principle is to investigate the performances of the solar concentrators taking into account the realistic solar coordinates and all the geometric and optical concentrator properties. Basing on a numerical model, the RT3D-4R method consist to follow-up a four solar incident rays since their exit from the solar disk until their interaction with the reflective collector surface and the absorbing receiver one.

3. Outcomes results

3.1. Shadows phenomena

In order to analyze the efficiency of the PTC system, it is interesting to examine all the possible optical phenomena occurred by interactions between solar incident rays, reflector aperture area, reflected rays and receiver area take into account the shading effects. The following flow chart describes the hitting probabilities by reflections, double reflections and triple reflections occurred between the directions of the reflected rays and the receiver out of the shadow of both reflector area and receiver area.



3.1.1. Hourly optical phenomena

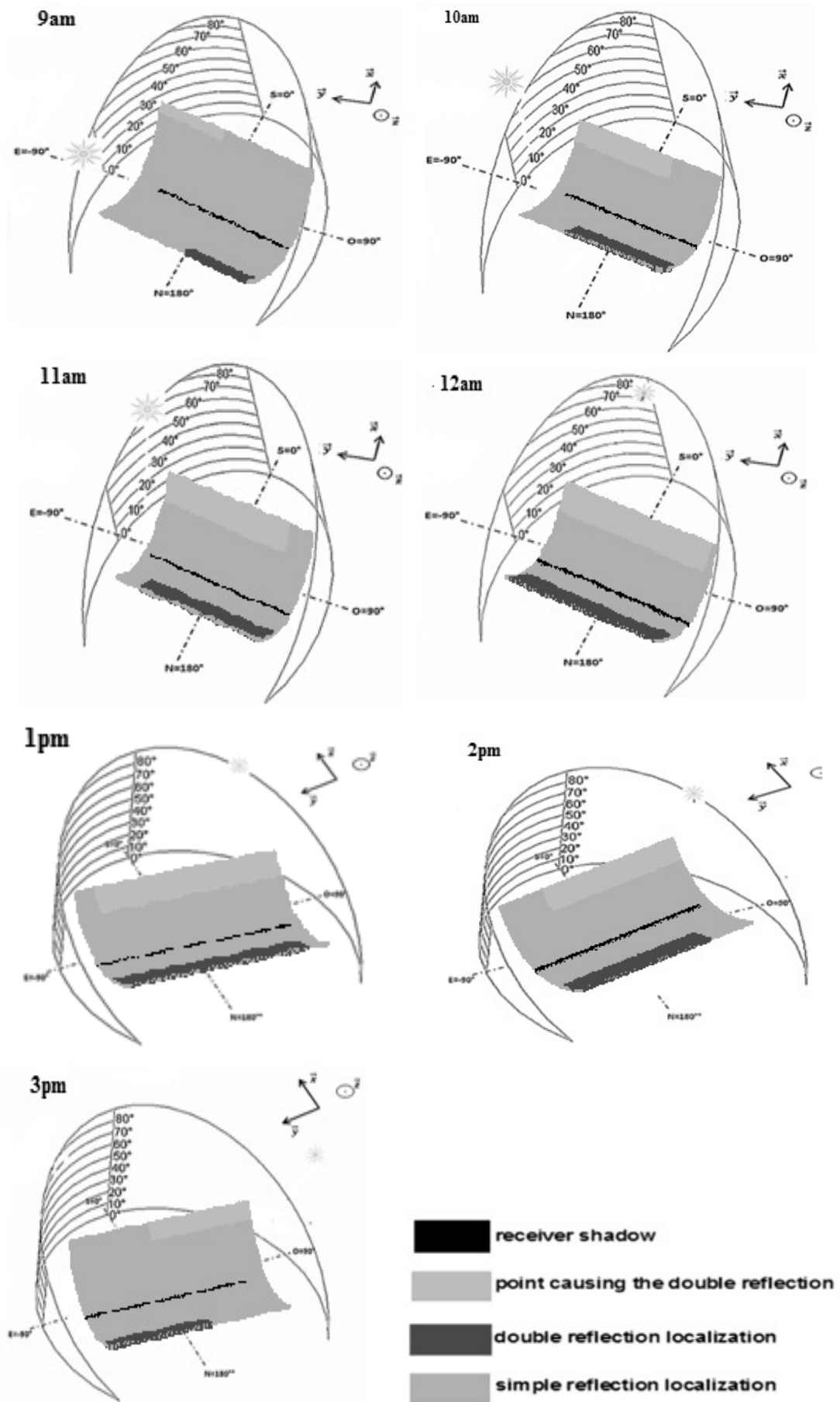


Figure 2: Hourly optical phenomena for E-W orientation for a fixed PTC system

Fig. 2 shows the hourly optical phenomena for E-W orientations for a fixed PTC system. It is clear that the distribution of the corresponding sizes and positions of each phenomenon differs from hour to another for each orientation. For an (E-W) orientation, the simple reflection phenomenon, marked by the argent color, is prevalent during the whole sampling hours while the double reflection phenomenon, marked by plumb color, occurs with lesser probability and therefore with smaller localization size on the reflector. Hence, a lower optical losses are achieved because a large number of incident rays can reach the absorber with simple reflections without undergoing further ones.

3.1.2. Hourly receiver shadow

Fig.3 illustrates the hourly receiver shadow position on the collector area for E-W orientation. One can observe that, despite the difference in the shadow surface length, the receiver shadow area (marked by the black color) has the same width relative to the cylindrical form of receiver. Therefore, we assume the same effective area on the collector. Concerning the hourly distribution of the receiver shadow, the hourly receiver shadows occurs almost in the same localization.

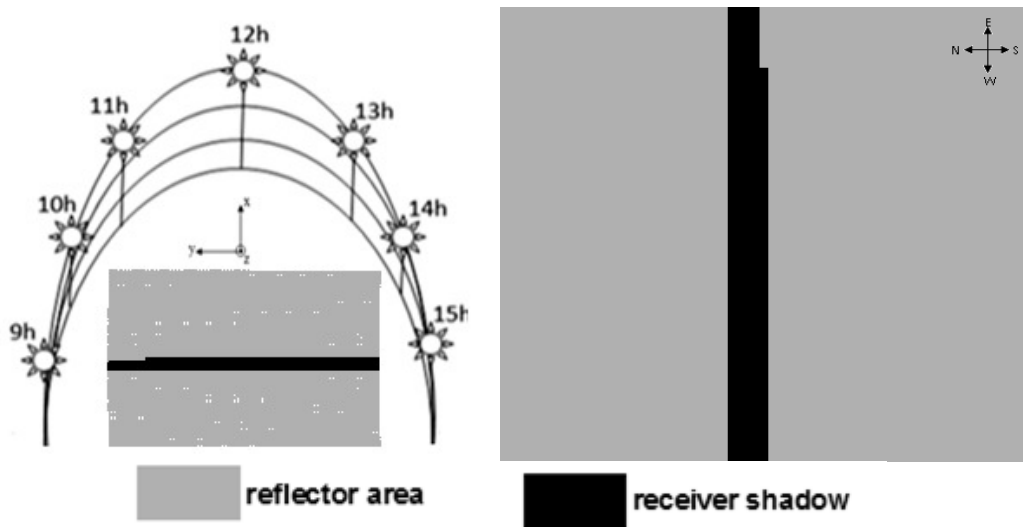


Figure 3: Hourly receiver shadow positions on the collector area for E-W PTC orientations

3.2. The tracked receiver system

From mathematic point of view, without normal sun incidence, the reflected rays cannot be concentrated in a specific line for a fixed PTC reflector. So, a PTC system requires compulsory a tracking system to constantly maintain the orientation of the mirror towards the moving sun.

From optical point of view, the solar densities distributions on the focal plane at mid-day for (E-W) orientation for both cylindrical and parabolic reflector are shown in fig.4. In fact, it's clear that for the parabolic reflector case the solar density area is above 0.2m which is greater than the receiver tube diameter, therefore, the increasing of the optical losses witnessed by lower solar densities under the value of 86kW/m². However, for the cylindrical reflector case the solar density is localized in specific thin spot and the solar densities go over the value of 200kW/m².

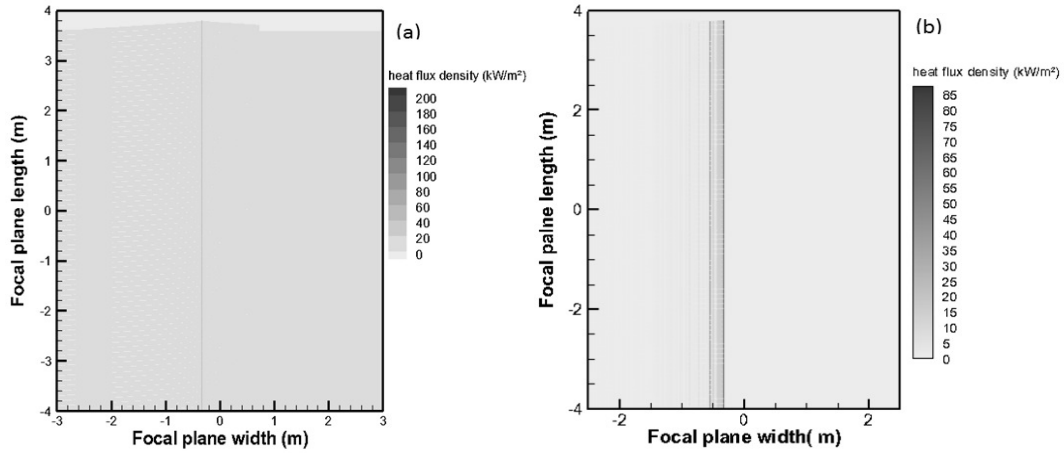


Figure 4: Solar density distribution on the focal plane for cylindrical reflector (a) and parabolic reflector (b)

Thus, in this present study, we will consider the reflector as cylindrical mirror because its geometry does not need to track the sun in any direction as long as some means is provided to intercept the moving focus. The equation of cylindrical mirror can be written as follows:

$$z = z_{cc} - \sqrt{r_c^2 - (x - x_{cc})^2} \quad (6)$$

In fact, we will focus on investigating the tracked receiver technique in the case of a fixed cylindrical reflector to further reduction of the concentrator tracking cost and use of small receiver sizes for a fixed solar concentrator.

Since the receiver is placed in the focal region, for a fixed system, the further away the receiver is, the more divergent the reflected solar rays and the concentrated solar energy become. Therefore, there must exist a critical location or position where the receiver captures the most amounts of reflected solar rays.

To determine these critical positions of the absorber tube, we consider a focus plane which corresponds to the optimal height of receiver covering the entire aperture and for each hour, the maximum of heat density corresponding to the optimal coordinates can be identified. Fig.5 shows a schematic displacement of the receiver position on the focal plane in term of the solar incident angle.

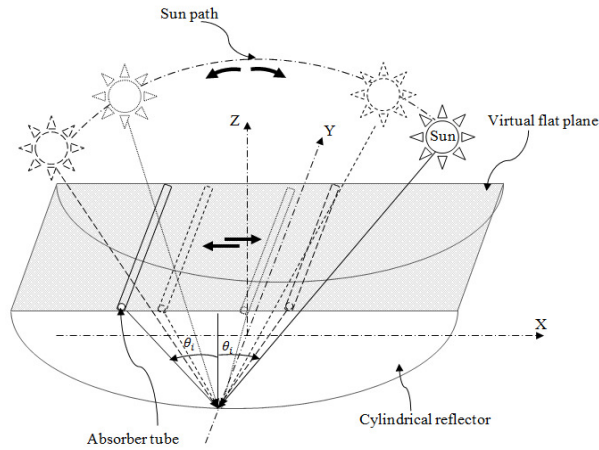
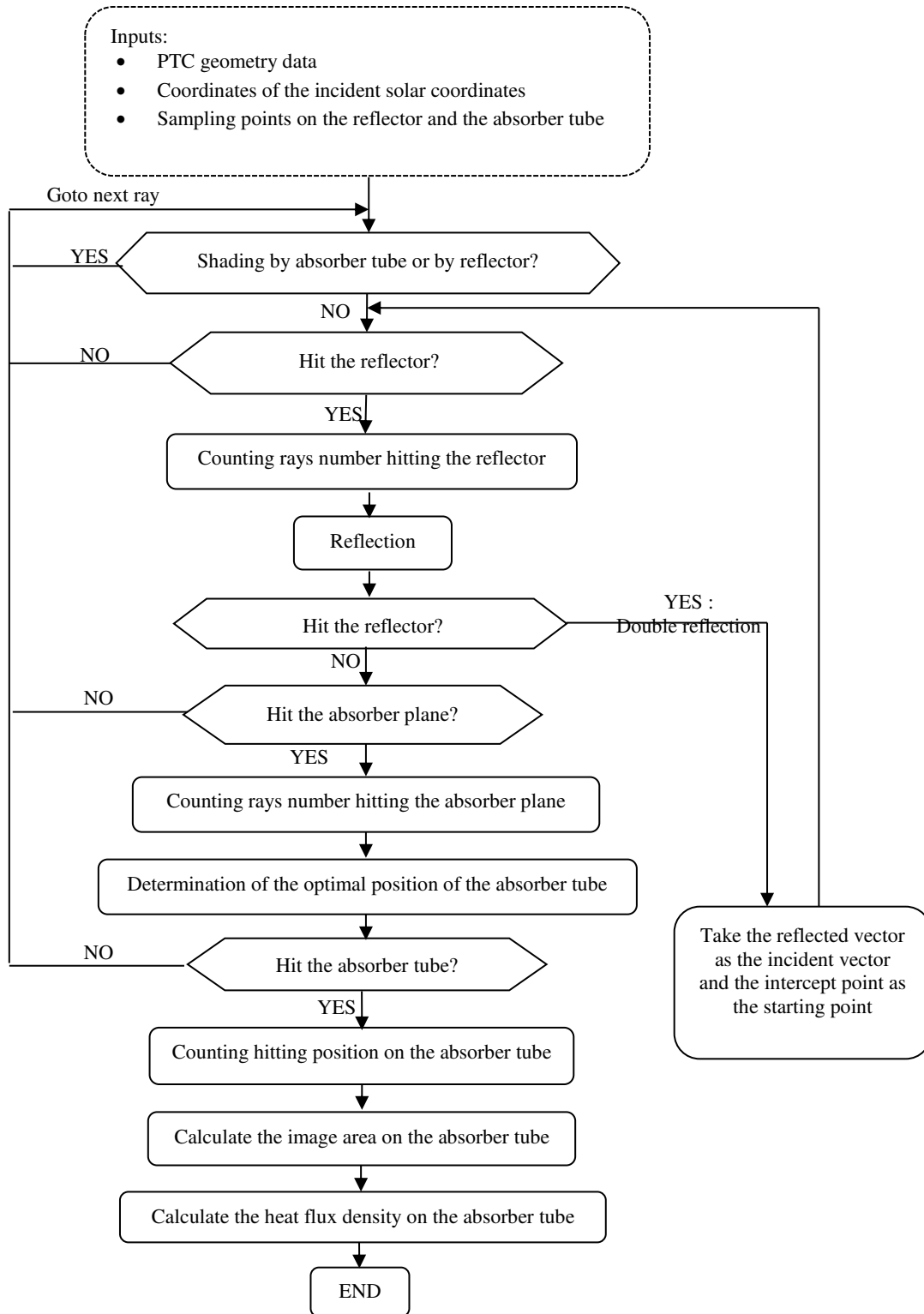


Figure 5: 3D schematic of receiver displacement shown in 3D

In order to determine the optimal positions of the absorber tube for the tracked receiver system, the following flow chart explains the different steps of computation:



When the fixed spherical collector is exposed to the sun, incident rays are reflected onto the tracked receiver tube. The collector is orientated in an (E-W) direction, moving the tracked receiver from north to south. Fig.6 shows the hourly 3D heat density distribution along the tracked receiver tube. It's clear that the maximum density is obtained at mid-day reaching the value of 151.145kW/m^2 .

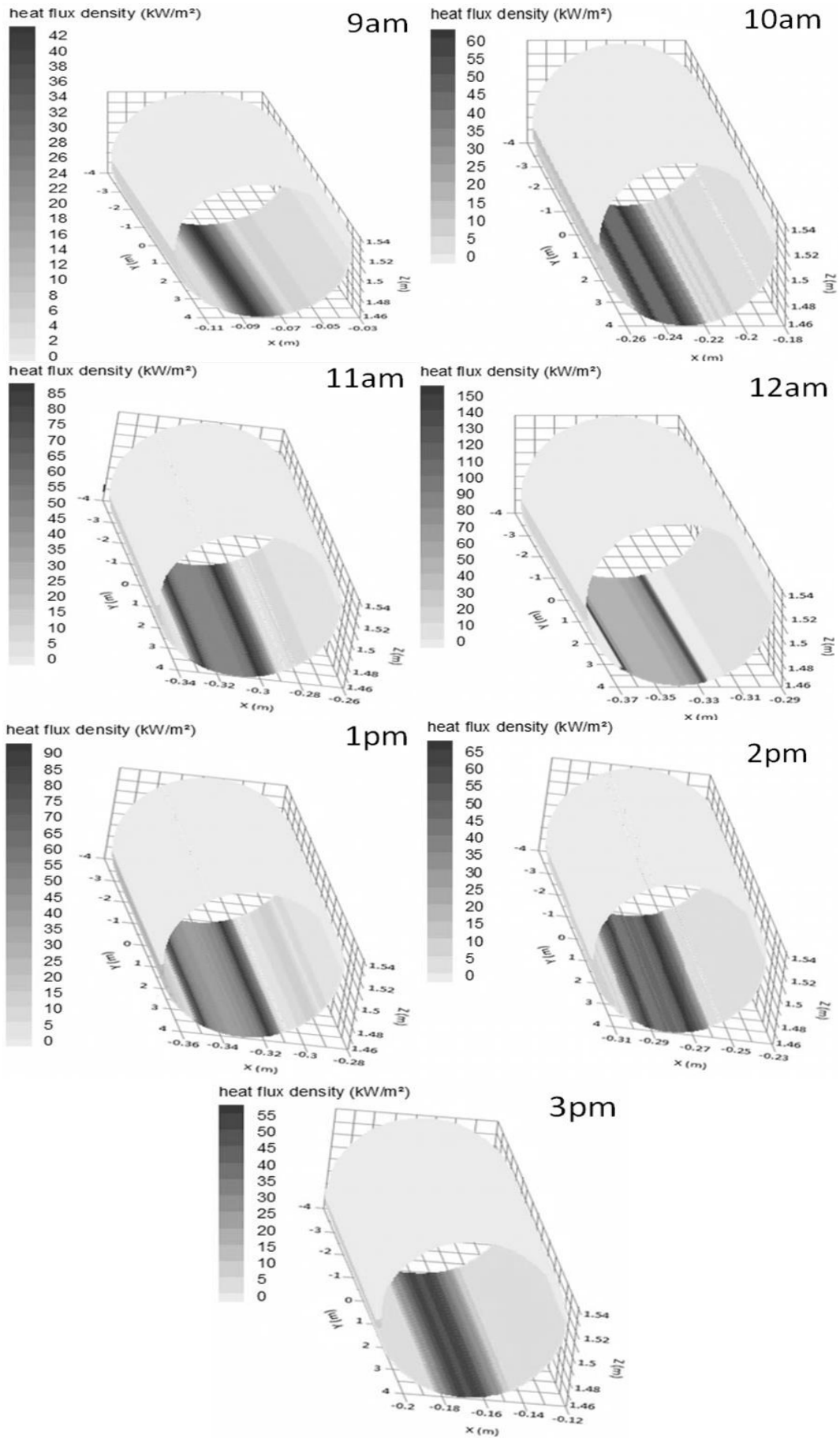


Figure 6: Hourly 3D heat density distribution along the tracked receiver tube

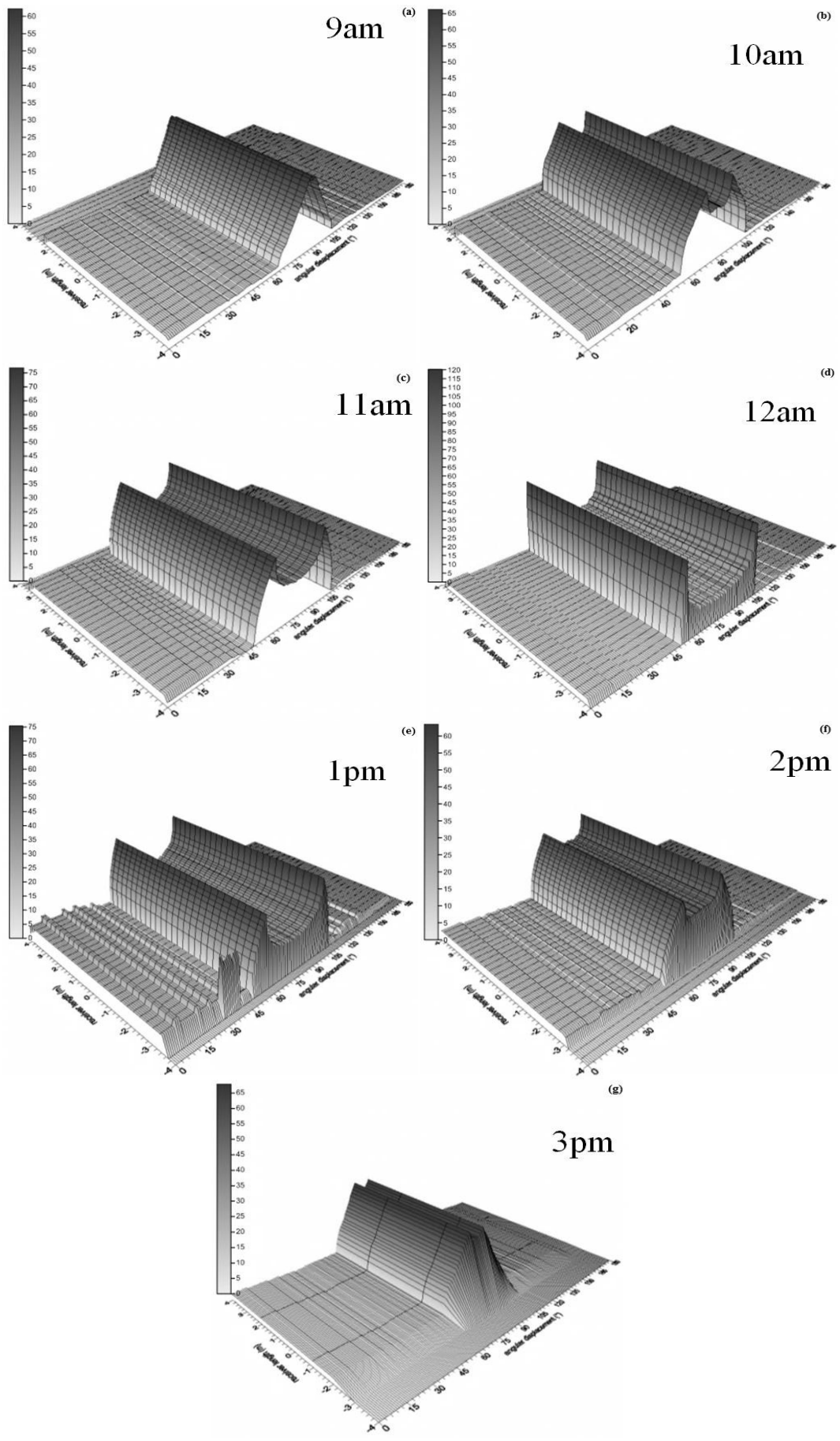


Figure 7: 3D hourly LCR distribution along the tracked receiver tube

The local concentration ratio is defined as the ratio of the solar flux density at a local position on the receiver surface to the incident solar irradiance [15].

$$LCR = \frac{Q_s(i, j)}{E_s} \quad (7)$$

Fig.7 show the 3D LCR hourly distribution on the tracked receiver tube for the optimal positions and for an (E-W) orientation. It's clear that the LCR distribution is characterized by its uniformity along the absorber tubes. Here, one can notice that the hourly variation of the span angle of the heat flux increasing zone with the solar zenith angle. In fact, the maximum of LCR is achieved at mid-day reaching the value of 120.24.

The one-axis tracked PTC system ensures the rotation from top to bottom in order to make the normal to the PTC aperture follows the angular height of the sun. The comparison between the LCR distribution on the receiver, of both tracked receiver system and one-axis tracked reflector system, is shown in Figs.8. One can notice that the LCR distribution curves, which have the same trend of variation as found by [16-20], are characterized by a non-uniform aspect in circle direction. As shown in figs.8, for one-axis tracked PTC system, the LCR keep the same tendency of variation for all the hours in term of amplitude and magnitude without exceeding the value of 60. In this case of tracking system, the LCR curve can be divided in four zones; (1): the shadow receiver zone, the hourly LCR curves show lower values. This is due to the solar angular radius which allows the reflected rays intercept the receiver at $\psi = 90^\circ$, even if the receiver tube is placed in the symmetrical axis of the reflector, (2): the heat flux increasing zone where the curves show a steady increase because the large number of reflected rays reaching the absorber in this angular interval. The hourly LCR maximums are obtained for ψ equal to 145° , (3): the heat flux decreasing zone where the LCR decreases because all the reflected rays will be tangent at the receiver in this angular position, (4): the beam radiation zone where the solar rays reach the receiver directly without being concentrated by the reflector. However, the shape of the LCR curves for the tracking receiver PTC system is different in comparison with those obtained by one-axis tracked system. In fact, there is no shadow receiver zone due to the real incidence of solar rays and the displacement of the receiver from the focus position. In contrast with the LCR curves of the first case of tracking, the LCR curves obtained by a tracked receiver PTC system are asymmetric. Also, one can observe that the span angle of the heat flux increasing zone increase with the decreasing of solar zenith angle. Moreover, the maximum LCR can be recorded at mid-day reaching the value of 120.24 which is more than three times those obtained by a one-axis tracked system.

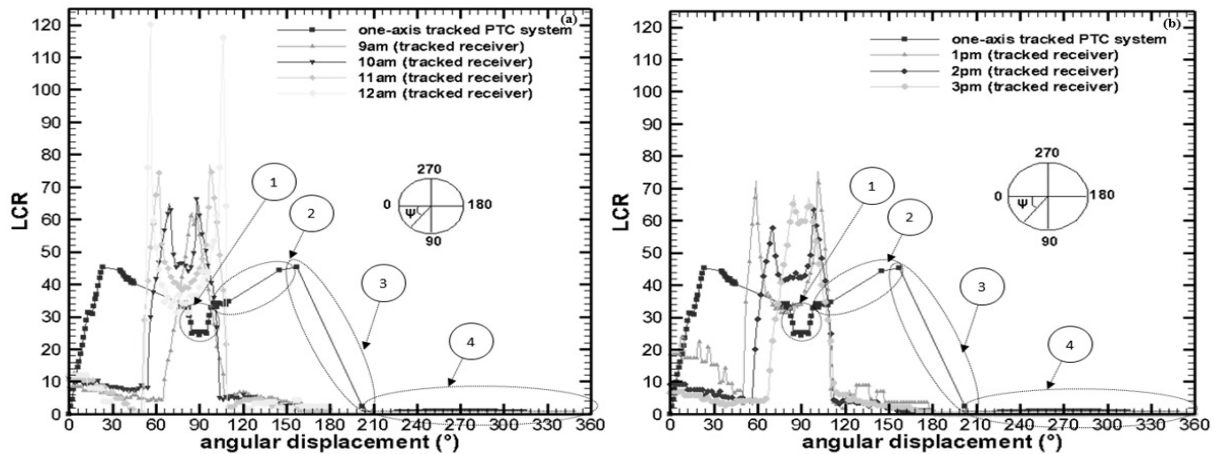


Figure 8: hourly LCR distribution for both tracked receiver system and one axis-tracked PTC system; for the morning (a) and for the afternoon (b)

Conclusion

In this paper, the performance of a PTC solar concentrating system has been investigated. A numerical method called RT 3D-4R has been used in order to study the optical concentration characteristics of the solar concentrator design using the case study of Monastir, some conclusions can be cited:

- The determination of the hourly optical phenomena for E-W orientation of a fixed PTC shows lower optical losses due to the dominance of the simple reflection area due to the big number of incidents rays which reach the absorber with only simple reflections.

- The study of the hourly distribution of the receiver shadow for E-W orientation of a fixed PTC indicates that, the hourly receiver shadows occurs almost in the same localization.
- Basing on a half solar angular radius equal to 16 arc-minutes, the optimal hourly heat concentrated solar density and LCR for tracked receiver are obtained at mid-day and reaching respectively 151.145kW/m² and 120.24.
- Basing on the heat hourly concentrated solar densities distribution along the receiver tube, a comparison between the E-W tracked receiver system orientation and the one-axis tracked PTC system has been analyzed in term of hourly LCR. This analysis indicates that both the concentrated solar density and LCR values for the tracked receiver system are higher than those achieved by the one-axis tracked PTC.

Nomenclature

Symbols	Name, <i>unit</i>	x, y, z	square coordinates
D	heat solar density, <i>kW/m²</i>	Greek symbols	
DNI	Direct Normal Irradiations, <i>kW/m²</i>	α	absorptivity of receiver tube
dS	elementary surface, <i>m²</i>	ρ	reflectivity of the reflector
ds	elementary heat solar density, <i>kW/m²</i>	σ	solar angular radius, <i>arc-minute</i>
ξ	insolation, <i>kW/m²</i>	τ	transmissivity of the glass envelope
E	East	ψ	angular displacement, $^{\circ}$
f	focal distance, <i>m</i>	Exponent, Indices	
i	incident ray	a	absorber
L	length, <i>m</i>	c	collector
LCR	Local Concentration Ratio	cc	collector center
n	normal on the reflector	cr	receiver center
N	North	eff	effective
PTC	Parabolic Trough Concentrator	i	incident
Q	solar flux, <i>kW</i>	r	receiver
r	radius, <i>m</i>	s, sun	solar
RT3D4R	Ray Tracing Three Dimension		
Four Rays			
S	South		
w	width, <i>m</i>		
W	West		

References

- [1] Abhijit Kumar Bhagat and M C Chattopadhyay, An Analysis on Solar Trackers a Potential Need for Future Solar Power Growth in India, *IJSRD - International Journal for Scientific Research & Development*, volume 4: pages 141-144, 2016.
- [2] Soteris A. Kalogirou, Solar thermal collectors and applications, *Progress in Energy and Combustion Science*, volume 30, pages 231–295, 2004.
- [3] Amr E. Gaafar and Ahmed F. Zobaa, Economical Design of a Two-Axis Tracking System for Solar Collectors, *5th IET Renewable Power Generation Conference (RPG 2016)*, London, 21 - 23 September 2016.
- [4] Kupta KC, Mirakhur PK, Sathe AP, A simple solar tracking system, *SUN Proceedings of the International Solar Energy Society*, New Delhi, India: Pergamon Press 1978.
- [5] Cope NA, Ingle HA, Farber EA, Morrison CA, Dynamic response analysis of a solar powered heliotropic fluid mechanical drive system, *University of Florida* 1981.
- [6] Singh TAK, Dinesh PS, Liquid vapour balance based sun tracking system, *Proceedings of the 25th National Renewable Energy Convention 2001 of the Solar Society of India*, Warangal, India 2001.
- [7] Cunxu Wang, Hongli Zhang and Shuqun Wang, Track Mode Selection of Parabolic Trough Collectors, *Advanced Science and Technology Letters*, volume 73, pages 52-59, 2014.
- [8] Stine WB, Harrigan RW, Solar energy fundamentals and design. New York: Wiley; 1985.
- [9] Hurt R, Yim W, Boehm R, Hale MJ, Gee R, Advanced parabolic trough field testing – real-time data collection, archiving, and analysis for the solar genix advanced parabolic trough, *International Solar Energy Conference*, Denver, Colorado July 2006.
- [10] Shortis MR, Johnston GHG, Pottler K, Lüpfer E, Remote sensing and spatial information sciences, *Int Arch Photogramm*; volume 37, pages 81–87, 2008
- [11] Saad Almonnieay, Robert Blaskey, Daniel Chief, Christopher, Mesko, Jairo Rivera, and Jacob Seitzer, Parabolic Trough-Tracking System, Problem Definition and Project Plan, *Northern Arizona University* 2014.

- [12] Puramanathan Naidoo, Theo I. van Niekerk, Optimising position control of a solar parabolic trough, *South Africa Journal of Science*; volume 107, 2011.
- [13] Evans D. On the Performance of Cylindrical Parabolic Solar Concentrators with Flat Absorbers, *Solar Energy*; volume 19, pages 379–385, 1977.
- [14] Houcine A, Maatallah T, El Alimi S, Ben Nasrallah S, The Performance Study of Parabolic Trough Concentrator Using a New RT3D-4R Method, *IJCTA*; volume 9, pages 133-139, 2016.
- [15] William B. Stine and Michael Geyer. Power From The Sun, chapter 8, 2001.
- [16] Hachicha, A. A., Rodríguez, I., Capdevila, R., Oliva, A., Heat transfer analysis and numerical simulation of a parabolic trough solar collector, *Applied Energy*, volume 111, pages 581–592, 2013.
- [17] He, Y. L., Xiao, J., Cheng, Z. D., Tao, Y. B., A MCRT and FVM coupled simulation method for energy conversion process in parabolic trough solar collector, *Renewable Energy*; volume 36, pages 976-985, 2011.
- [18] Jeter, M. S., Calculation of the concentrated flux density distribution in parabolic trough collectors by a semi finite formulation, *Solar Energy*; volume 37, pages 335-345, 1986.
- [19] Aggrey Mwesigye , Tunde Bello-Ochende , Josua P. Meyer, Minimum entropy generation due to heat transfer and fluid friction in a parabolic trough receiver with non-uniform heat flux at different rim angles and concentration ratio, *Energy*; volume 73, pages 606-617, 2014.
- [20] Yang B, Zhao J, Xu T, Zhu Q. Calculation of the concentrated flux density distribution in parabolic trough solar concentrators by Monte Carlo ray-trace method, *In: Photonics and optoelectronic (SOPO)*, pages 1-4, 2010.

25-27 Octobre 2017
Monastir - Tunisie